

Direct Measurement of the Branching Fractions $\mathcal{B}(\psi(3686) \rightarrow J/\psi X)$ and $\mathcal{B}(\psi(3770) \rightarrow J/\psi X)$, and Observation of the State $\mathcal{R}(3760)$ in $e^+e^- \rightarrow J/\psi X$

M. Ablikim,¹ M. N. Achasov,^{10,e} P. Adlarson,⁶³ S. Ahmed,¹⁵ M. Albrecht,⁴ A. Amoroso,^{62a,62c} Q. An,^{59,47} Anita,²¹ Y. Bai,⁴⁶ O. Bakina,²⁸ R. Baldini Ferroli,^{23a} I. Balossino,^{24a} Y. Ban,^{37,m} K. Begzsuren,²⁶ J. V. Bennett,⁵ N. Berger,²⁷ M. Bertani,^{23a} D. Bettoni,^{24a} F. Bianchi,^{62a,62c} J. Biernat,⁶³ J. Bloms,⁵⁶ A. Bortone,^{62a,62c} I. Boyko,²⁸ R. A. Briere,⁵ H. Cai,⁶⁴ X. Cai,^{1,47} A. Calcaterra,^{23a} G. F. Cao,^{1,51} N. Cao,^{1,51} S. A. Cetin,^{50b} J. F. Chang,^{1,47} W. L. Chang,^{1,51} G. Chelkov,^{28,c,d} D. Y. Chen,⁶ G. Chen,¹ H. S. Chen,^{1,51} M. L. Chen,^{1,47} S. J. Chen,³⁵ X. R. Chen,²⁵ Y. B. Chen,^{1,47} W. Cheng,^{62c} G. Cibinetto,^{24a} F. Cossio,^{62c} X. F. Cui,³⁶ H. L. Dai,^{1,47} J. P. Dai,^{41,i} X. C. Dai,^{1,51} A. Dbeysy,¹⁵ R. B. de Boer,⁴ D. Dedovich,²⁸ Z. Y. Deng,¹ A. Denig,²⁷ I. Denysenko,²⁸ M. Destefanis,^{62a,62c} F. De Mori,^{62a,62c} Y. Ding,³³ C. Dong,³⁶ J. Dong,^{1,47} L. Y. Dong,^{1,51} M. Y. Dong,^{1,47,51} S. X. Du,⁶⁷ J. Fang,^{1,47} S. S. Fang,^{1,51} Y. Fang,¹ R. Farinelli,^{24a,24b} L. Fava,^{62b,62c} F. Feldbauer,⁴ G. Felici,^{23a} C. Q. Feng,^{59,47} M. Fritsch,⁴ C. D. Fu,¹ Y. Fu,¹ X. L. Gao,^{59,47} Y. Gao,⁶⁰ Y. Gao,^{37,m} Y. G. Gao,⁶ I. Garzia,^{24a,24b} E. M. Gersabeck,⁵⁴ A. Gilman,⁵⁵ K. Goetzen,¹¹ L. Gong,³⁶ W. X. Gong,^{1,47} W. Gradl,²⁷ M. Greco,^{62a,62c} L. M. Gu,³⁵ M. H. Gu,^{1,47} S. Gu,² Y. T. Gu,¹³ C. Y. Guan,^{1,51} A. Q. Guo,²² L. B. Guo,³⁴ R. P. Guo,³⁹ Y. P. Guo,^{9,j} Y. P. Guo,²⁷ A. Guskov,²⁸ S. Han,⁶⁴ T. T. Han,⁴⁰ T. Z. Han,^{9,j} X. Q. Hao,¹⁶ F. A. Harris,⁵² K. L. He,^{1,51} F. H. Heinsius,⁴ T. Held,⁴ Y. K. Heng,^{1,47,51} M. Himmelreich,^{11,h} T. Holtmann,⁴ Y. R. Hou,⁵¹ Z. L. Hou,¹ H. M. Hu,^{1,51} J. F. Hu,^{41,i} T. Hu,^{1,47,51} Y. Hu,¹ G. S. Huang,^{59,47} L. Q. Huang,⁶⁰ X. T. Huang,⁴⁰ Z. Huang,^{37,m} N. Huesken,⁵⁶ T. Hussain,⁶¹ W. Ikegami Andersson,⁶³ W. Imoehl,²² M. Irshad,^{59,47} S. Jaeger,⁴ S. Janchiv,^{26,i} Q. Ji,¹ Q. P. Ji,¹⁶ X. B. Ji,^{1,51} X. L. Ji,^{1,47} H. B. Jiang,⁴⁰ X. S. Jiang,^{1,47,51} X. Y. Jiang,³⁶ J. B. Jiao,⁴⁰ Z. Jiao,¹⁸ S. Jin,³⁵ Y. Jin,⁵³ T. Johansson,⁶³ N. Kalantar-Nayestanaki,³⁰ X. S. Kang,³³ R. Kappert,³⁰ M. Kavatsyuk,³⁰ B. C. Ke,^{42,1} I. K. Keshk,⁴ A. Khoukaz,⁵⁶ P. Kiese,²⁷ R. Kiuchi,¹ R. Kliemt,¹¹ L. Koch,²⁹ O. B. Kolcu,^{50b,g} B. Kopf,⁴ M. Kuemmel,⁴ M. Kuessner,⁴ A. Kupsc,⁶³ M. G. Kurth,^{1,51} W. Kühn,²⁹ J. J. Lane,⁵⁴ J. S. Lange,²⁹ P. Larin,¹⁵ L. Lavezzi,^{62c} H. Leithoff,²⁷ M. Lellmann,²⁷ T. Lenz,²⁷ C. Li,³⁸ C. H. Li,³² Cheng Li,^{59,47} D. M. Li,⁶⁷ F. Li,^{1,47} G. Li,¹ H. B. Li,^{1,51} H. J. Li,^{9,j} J. L. Li,⁴⁰ J. Q. Li,⁴ Ke Li,¹ L. K. Li,¹ Lei Li,³ P. L. Li,^{59,47} P. R. Li,³¹ S. Y. Li,⁴⁹ W. D. Li,^{1,51} W. G. Li,¹ X. H. Li,^{59,47} X. L. Li,⁴⁰ Z. B. Li,⁴⁸ Z. Y. Li,⁴⁸ H. Liang,^{59,47} H. Liang,^{1,51} Y. F. Liang,⁴⁴ Y. T. Liang,²⁵ L. Z. Liao,^{1,51} J. Libby,²¹ C. X. Lin,⁴⁸ B. Liu,^{41,i} B. J. Liu,¹ C. X. Liu,¹ D. Liu,^{59,47} D. Y. Liu,^{41,i} F. H. Liu,⁴³ Fang Liu,¹ Feng Liu,⁶ H. B. Liu,¹³ H. M. Liu,^{1,51} Huanhuan Liu,¹ Huihui Liu,¹⁷ J. B. Liu,^{59,47} J. Y. Liu,^{1,51} K. Liu,¹ K. Y. Liu,³³ Ke Liu,⁶ L. Liu,^{59,47} L. Y. Liu,¹³ Q. Liu,⁵¹ S. B. Liu,^{59,47} T. Liu,^{1,51} X. Liu,³¹ Y. B. Liu,³⁶ Z. A. Liu,^{1,47,51} Z. Q. Liu,⁴⁰ Y. F. Long,^{37,m} X. C. Lou,^{1,47,51} H. J. Lu,¹⁸ J. D. Lu,^{1,51} J. G. Lu,^{1,47} X. L. Lu,¹ Y. Lu,¹ Y. P. Lu,^{1,47} C. L. Luo,³⁴ M. X. Luo,⁶⁶ P. W. Luo,⁴⁸ T. Luo,^{9,j} X. L. Luo,^{1,47} S. Lusso,^{62c} X. R. Lyu,⁵¹ F. C. Ma,³³ H. L. Ma,¹ L. L. Ma,⁴⁰ M. M. Ma,^{1,51} Q. M. Ma,¹ R. Q. Ma,^{1,51} R. T. Ma,⁵¹ X. N. Ma,³⁶ X. X. Ma,^{1,51} X. Y. Ma,^{1,47} Y. M. Ma,⁴⁰ F. E. Maas,¹⁵ M. Maggiora,^{62a,62c} S. Maldaner,²⁷ S. Malde,⁵⁷ Q. A. Malik,⁶¹ A. Mangoni,^{23b} Y. J. Mao,^{37,m} Z. P. Mao,¹ S. Marcello,^{62a,62c} Z. X. Meng,⁵³ J. G. Messchendorp,³⁰ G. Mezzadri,^{24a} T. J. Min,³⁵ R. E. Mitchell,²² X. H. Mo,^{1,47,51} Y. J. Mo,⁶ N. Yu. Muchnoi,^{10,e} H. Muramatsu,⁵⁵ S. Nakhoul,^{11,h} Y. Nefedov,²⁸ F. Nerling,^{11,h} I. B. Nikolaev,^{10,e} Z. Ning,^{1,47} S. Nisar,^{8,k} S. L. Olsen,⁵¹ Q. Ouyang,^{1,47,51} S. Pacetti,^{23b} Y. Pan,⁵⁴ M. Papenbrock,⁶³ A. Pathak,¹ P. Patteri,^{23a} M. Pelizaeus,⁴ H. P. Peng,^{59,47} K. Peters,^{11,h} J. Pettersson,⁶³ J. L. Ping,³⁴ R. G. Ping,^{1,51} A. Pitka,⁴ R. Poling,⁵⁵ V. Prasad,^{59,47} H. Qi,^{59,47} H. R. Qi,⁴⁹ M. Qi,³⁵ T. Y. Qi,² S. Qian,^{1,47} W.-B. Qian,⁵¹ C. F. Qiao,⁵¹ L. Q. Qin,¹² X. P. Qin,¹³ X. S. Qin,⁴ Z. H. Qin,^{1,47} J. F. Qiu,¹ S. Q. Qu,³⁶ K. H. Rashid,⁶¹ K. Ravindran,²¹ C. F. Redmer,²⁷ A. Rivetti,^{62c} V. Rodin,³⁰ M. Rolo,^{62c} G. Rong,^{1,51} Ch. Rosner,¹⁵ M. Rump,⁵⁶ A. Sarantsev,^{28,f} M. Savrié,^{24b} Y. Schelhaas,²⁷ C. Schnier,⁴ K. Schoenning,⁶³ W. Shan,¹⁹ X. Y. Shan,^{59,47} M. Shao,^{59,47} C. P. Shen,² P. X. Shen,³⁶ X. Y. Shen,^{1,51} H. C. Shi,^{59,47} R. S. Shi,^{1,51} X. Shi,^{1,47} X. D. Shi,^{59,47} J. J. Song,⁴⁰ Q. Q. Song,^{59,47} Y. X. Song,^{37,m} S. Sosio,^{62a,62c} S. Spataro,^{62a,62c} F. F. Sui,⁴⁰ G. X. Sun,¹ J. F. Sun,¹⁶ L. Sun,⁶⁴ S. S. Sun,^{1,51} T. Sun,^{1,51} W. Y. Sun,³⁴ Y. J. Sun,^{59,47} Y. K. Sun,^{59,47} Y. Z. Sun,¹ Z. T. Sun,¹ Y. X. Tan,^{59,47} C. J. Tang,⁴⁴ G. Y. Tang,¹ J. Tang,⁴⁸ V. Thoren,⁶³ B. Tsednee,²⁶ I. Uman,^{50d} B. Wang,¹ B. L. Wang,⁵¹ C. W. Wang,³⁵ D. Y. Wang,^{37,m} H. P. Wang,^{1,51} K. Wang,^{1,47} L. L. Wang,¹ M. Wang,⁴⁰ M. Z. Wang,^{37,m} Meng Wang,^{1,51} W. P. Wang,^{59,47} X. Wang,^{37,m} X. F. Wang,³¹ X. L. Wang,^{9,j} Y. Wang,⁴⁸ Y. Wang,^{59,47} Y. D. Wang,¹⁵ Y. F. Wang,^{1,47,51} Y. Q. Wang,¹ Z. Wang,^{1,47} Z. Y. Wang,¹ Ziyi Wang,⁵¹ Zongyuan Wang,^{1,51} T. Weber,⁴ D. H. Wei,¹² P. Weidenkaff,²⁷ F. Weidner,⁵⁶ H. W. Wen,^{34,a} S. P. Wen,¹ D. J. White,⁵⁴ U. Wiedner,⁴ G. Wilkinson,⁵⁷ M. Wolke,⁶³ L. Wollenberg,⁴ J. F. Wu,^{1,51} L. H. Wu,¹ L. J. Wu,^{1,51} X. Wu,^{9,j} Z. Wu,^{1,47} L. Xia,^{59,47} H. Xiao,^{9,j} S. Y. Xiao,¹ Y. J. Xiao,^{1,51} Z. J. Xiao,³⁴ X. H. Xie,^{37,m} Y. G. Xie,^{1,47} Y. H. Xie,⁶ T. Y. Xing,^{1,51} X. A. Xiong,^{1,51} G. F. Xu,¹ J. J. Xu,³⁵ Q. J. Xu,¹⁴ W. Xu,^{1,51} X. P. Xu,⁴⁵ L. Yan,^{9,j} L. Yan,^{62a,62c} W. B. Yan,^{59,47} W. C. Yan,⁶⁷ H. J. Yang,^{41,i} H. X. Yang,¹ L. Yang,⁶⁴ R. X. Yang,^{59,47} S. L. Yang,^{1,51} Y. H. Yang,³⁵ Y. X. Yang,¹²

Yifan Yang,^{1,51} Zhi Yang,²⁵ M. Ye,^{1,47} M. H. Ye,⁷ J. H. Yin,¹ Z. Y. You,⁴⁸ B. X. Yu,^{1,47,51} C. X. Yu,³⁶ G. Yu,^{1,51} J. S. Yu,^{20,n}
 T. Yu,⁶⁰ C. Z. Yuan,^{1,51} W. Yuan,^{62a,62c} X. Q. Yuan,^{37,m} Y. Yuan,¹ C. X. Yue,³² A. Yuncu,^{50b,b} A. A. Zafar,⁶¹ Y. Zeng,^{20,n}
 B. X. Zhang,¹ Guangyi Zhang,¹⁶ H. H. Zhang,⁴⁸ H. Y. Zhang,^{1,47} J. L. Zhang,⁶⁵ J. Q. Zhang,⁴ J. W. Zhang,^{1,47,51}
 J. Y. Zhang,¹ J. Z. Zhang,^{1,51} Jianyu Zhang,^{1,51} Jiawei Zhang,^{1,51} L. Zhang,¹ Lei Zhang,³⁵ S. Zhang,⁴⁸ S. F. Zhang,³⁵
 T. J. Zhang,^{41,i} X. Y. Zhang,⁴⁰ Y. Zhang,⁵⁷ Y. H. Zhang,^{1,47} Y. T. Zhang,^{59,47} Yan Zhang,^{59,47} Yao Zhang,¹ Yi Zhang,^{9,j}
 Z. H. Zhang,⁶ Z. Y. Zhang,⁶⁴ G. Zhao,¹ J. Zhao,³² J. Y. Zhao,^{1,51} J. Z. Zhao,^{1,47} Lei Zhao,^{59,47} Ling Zhao,¹ M. G. Zhao,³⁶
 Q. Zhao,¹ S. J. Zhao,⁶⁷ Y. B. Zhao,^{1,47} Y. X. Zhao Zhao,²⁵ Z. G. Zhao,^{59,47} A. Zhemchugov,^{28,c} B. Zheng,⁶⁰ J. P. Zheng,^{1,47}
 Y. Zheng,^{37,m} Y. H. Zheng,⁵¹ B. Zhong,³⁴ C. Zhong,⁶⁰ L. P. Zhou,^{1,51} Q. Zhou,^{1,51} X. Zhou,⁶⁴ X. K. Zhou,⁵¹ X. R. Zhou,^{59,47}
 A. N. Zhu,^{1,51} J. Zhu,³⁶ K. Zhu,¹ K. J. Zhu,^{1,47,51} S. H. Zhu,⁵⁸ W. J. Zhu,³⁶ X. L. Zhu,⁴⁹ Y. C. Zhu,^{59,47} Z. A. Zhu,^{1,51}
 B. S. Zou,¹ and J. H. Zou¹

(BESIII Collaboration)

¹*Institute of High Energy Physics, Beijing 100049, People's Republic of China*²*Beihang University, Beijing 100191, People's Republic of China*³*Beijing Institute of Petrochemical Technology, Beijing 102617, People's Republic of China*⁴*Bochum Ruhr-University, D-44780 Bochum, Germany*⁵*Carnegie Mellon University, Pittsburgh, Pennsylvania 15213, USA*⁶*Central China Normal University, Wuhan 430079, People's Republic of China*⁷*China Center of Advanced Science and Technology, Beijing 100190, People's Republic of China*⁸*COMSATS University Islamabad, Lahore Campus, Defence Road, Off Raiwind Road, 54000 Lahore, Pakistan*⁹*Fudan University, Shanghai 200443, People's Republic of China*¹⁰*G. I. Budker Institute of Nuclear Physics SB RAS (BINP), Novosibirsk 630090, Russia*¹¹*GSI Helmholtzcentre for Heavy Ion Research GmbH, D-64291 Darmstadt, Germany*¹²*Guangxi Normal University, Guilin 541004, People's Republic of China*¹³*Guangxi University, Nanning 530004, People's Republic of China*¹⁴*Hangzhou Normal University, Hangzhou 310036, People's Republic of China*¹⁵*Helmholtz Institute Mainz, Johann-Joachim-Becher-Weg 45, D-55099 Mainz, Germany*¹⁶*Henan Normal University, Xinxiang 453007, People's Republic of China*¹⁷*Henan University of Science and Technology, Luoyang 471003, People's Republic of China*¹⁸*Huangshan College, Huangshan 245000, People's Republic of China*¹⁹*Hunan Normal University, Changsha 410081, People's Republic of China*²⁰*Hunan University, Changsha 410082, People's Republic of China*²¹*Indian Institute of Technology Madras, Chennai 600036, India*²²*Indiana University, Bloomington, Indiana 47405, USA*^{23a}*INFN Laboratori Nazionali di Frascati, I-00044 Frascati, Italy*^{23b}*INFN and University of Perugia, I-06100 Perugia, Italy*^{24a}*INFN Sezione di Ferrara, I-44122 Ferrara, Italy*^{24b}*University of Ferrara, I-44122 Ferrara, Italy*²⁵*Institute of Modern Physics, Lanzhou 730000, People's Republic of China*²⁶*Institute of Physics and Technology, Peace Avenue 54B, Ulaanbaatar 13330, Mongolia*²⁷*Johannes Gutenberg University of Mainz, Johann-Joachim-Becher-Weg 45, D-55099 Mainz, Germany*²⁸*Joint Institute for Nuclear Research, 141980 Dubna, Moscow region, Russia*²⁹*Justus-Liebig-Universitaet Giessen, II. Physikalisches Institut, Heinrich-Buff-Ring 16, D-35392 Giessen, Germany*³⁰*KVI-CART, University of Groningen, NL-9747 AA Groningen, Netherlands*³¹*Lanzhou University, Lanzhou 730000, People's Republic of China*³²*Liaoning Normal University, Dalian 116029, People's Republic of China*³³*Liaoning University, Shenyang 110036, People's Republic of China*³⁴*Nanjing Normal University, Nanjing 210023, People's Republic of China*³⁵*Nanjing University, Nanjing 210093, People's Republic of China*³⁶*Nankai University, Tianjin 300071, People's Republic of China*³⁷*Peking University, Beijing 100871, People's Republic of China*³⁸*Qufu Normal University, Qufu 273165, People's Republic of China*³⁹*Shandong Normal University, Jinan 250014, People's Republic of China*⁴⁰*Shandong University, Jinan 250100, People's Republic of China*⁴¹*Shanghai Jiao Tong University, Shanghai 200240, People's Republic of China*⁴²*Shanxi Normal University, Linfen 041004, People's Republic of China*⁴³*Shanxi University, Taiyuan 030006, People's Republic of China*

- ⁴⁴Sichuan University, Chengdu 610064, People's Republic of China
⁴⁵Soochow University, Suzhou 215006, People's Republic of China
⁴⁶Southeast University, Nanjing 211100, People's Republic of China
⁴⁷State Key Laboratory of Particle Detection and Electronics, Beijing 100049, Hefei 230026, People's Republic of China
⁴⁸Sun Yat-Sen University, Guangzhou 510275, People's Republic of China
⁴⁹Tsinghua University, Beijing 100084, People's Republic of China
^{50a}Ankara University, 06100 Tandogan, Ankara, Turkey
^{50b}Istanbul Bilgi University, 34060 Eyup, Istanbul, Turkey
^{50c}Uludag University, 16059 Bursa, Turkey
^{50d}Near East University, Nicosia, North Cyprus, Mersin 10, Turkey
⁵¹University of Chinese Academy of Sciences, Beijing 100049, People's Republic of China
⁵²University of Hawaii, Honolulu, Hawaii 96822, USA
⁵³University of Jinan, Jinan 250022, People's Republic of China
⁵⁴University of Manchester, Oxford Road, Manchester M13 9PL, United Kingdom
⁵⁵University of Minnesota, Minneapolis, Minnesota 55455, USA
⁵⁶University of Muenster, Wilhelm-Klemm-Strasse 9, 48149 Muenster, Germany
⁵⁷University of Oxford, Keble Road, Oxford OX13RH, United Kingdom
⁵⁸University of Science and Technology Liaoning, Anshan 114051, People's Republic of China
⁵⁹University of Science and Technology of China, Hefei 230026, People's Republic of China
⁶⁰University of South China, Hengyang 421001, People's Republic of China
⁶¹University of the Punjab, Lahore-54590, Pakistan
^{62a}University of Turin, I-10125 Turin, Italy
^{62b}University of Eastern Piedmont, I-15121 Alessandria, Italy
^{62c}INFN, I-10125 Turin, Italy
⁶³Uppsala University, Box 516, SE-75120 Uppsala, Sweden
⁶⁴Wuhan University, Wuhan 430072, People's Republic of China
⁶⁵Xinyang Normal University, Xinyang 464000, People's Republic of China
⁶⁶Zhejiang University, Hangzhou 310027, People's Republic of China
⁶⁷Zhengzhou University, Zhengzhou 450001, People's Republic of China

 (Received 20 November 2020; revised 21 June 2021; accepted 13 July 2021; published 19 August 2021)

We report a measurement of the observed cross sections of $e^+e^- \rightarrow J/\psi X$ based on 3.21 fb^{-1} of data accumulated at energies from 3.645 to 3.891 GeV with the BESIII detector operated at the BEPCII collider. In analysis of the cross sections, we measured the decay branching fractions of $\mathcal{B}(\psi(3686) \rightarrow J/\psi X) = (64.4 \pm 0.6 \pm 1.6)\%$ and $\mathcal{B}(\psi(3770) \rightarrow J/\psi X) = (0.5 \pm 0.2 \pm 0.1)\%$ for the first time. The energy-dependent line shape of these cross sections cannot be well described by two Breit-Wigner (BW) amplitudes of the expected decays $\psi(3686) \rightarrow J/\psi X$ and $\psi(3770) \rightarrow J/\psi X$. Instead, it can be better described with one more BW amplitude of the decay $\mathcal{R}(3760) \rightarrow J/\psi X$. Under this assumption, we extracted the $\mathcal{R}(3760)$ mass $M_{\mathcal{R}(3760)} = 3766.2 \pm 3.8 \pm 0.4 \text{ MeV}/c^2$, total width $\Gamma_{\mathcal{R}(3760)}^{\text{tot}} = 22.2 \pm 5.9 \pm 1.4 \text{ MeV}$, and product of leptonic width and decay branching fraction $\Gamma_{\mathcal{R}(3760)}^{ee} \mathcal{B}[\mathcal{R}(3760) \rightarrow J/\psi X] = (79.4 \pm 85.5 \pm 11.7) \text{ eV}$. The significance of the $\mathcal{R}(3760)$ is 5.3σ . The first uncertainties of these measured quantities are from fits to the cross sections and second systematic.

DOI: [10.1103/PhysRevLett.127.082002](https://doi.org/10.1103/PhysRevLett.127.082002)

The mesons with mass above the threshold of open-charm (OC) pairs had been considered for more than 25 years to decay entirely to OC final states via the strong interaction. Only a few experimental studies of non-OC (NOC) decays

of these mesons had been carried out before the summer of 2002 [1,2]. In July 2003, the BES Collaboration claimed for the first time that they had observed 7 ± 3 events of the NOC final state of $J/\psi\pi^+\pi^-$ [3] in the e^+e^- collision data taken with the BES-II detector operated at the BEPC collider at center-of-mass (c.m.) energies near 3.773 GeV. This observation started worldwide a new era with the aim to study rigorously NOC decays of the mesons lying above OC thresholds. After more than two years of intensive discussion in the particle physics community about whether the $J/\psi\pi^+\pi^-$ final state is really a decay product of the mesons

Published by the American Physical Society under the terms of the [Creative Commons Attribution 4.0 International license](https://creativecommons.org/licenses/by/4.0/). Further distribution of this work must maintain attribution to the author(s) and the published article's title, journal citation, and DOI. Funded by SCOAP³.

lying above the lowest OC threshold (3.73 GeV), it has been accepted that this golden final state is a product of the $\psi(3770)$ NOC decays. However, it has not been excluded that this golden final state may be a decay product of some other possible structures [4] which was speculated to exist in this energy region. The discovery of the first NOC final state of $J/\psi\pi^+\pi^-$ from the meson(s) decays overturns the conventional knowledge that almost 100% of the mesons decay into OC final states through the strong interaction [5]. It stimulated a strong interest in studying NOC decays of the mesons lying above the OC thresholds, and it inspired more experimental efforts at the e^+e^- experiments to study NOC decays of the mesons [1,5,6]. In particular, the study of the $J/\psi\pi^+\pi^-$ final state or a similar final state such as $M_{c\bar{c}}X_{\text{LH}}$ [$M_{c\bar{c}}$ is a hidden charm meson such as J/ψ , $\psi(3686)$, $\chi_{cJ}(J=0,1,2)$, and h_c , while X_{LH} refers to any allowed light hadron(s)] and the $\mu^+\mu^-$ final state [5,7] leads to the discovery of several new states [8–11], such as the historically labeled X , Y , and Z states.

The potential model [12] expects that $\psi(3770)$ is the only $c\bar{c}$ state, which can be directly produced in e^+e^- annihilation at energies from 3.73 to 3.87 GeV and decay to OC pairs with a branching fraction exceeding 99%. However, the BES found [13–16] about $(16.4 \pm 7.3 \pm 4.2)\%$ of $\psi(3770)$ decaying to NOC final states, which indicates that the $\psi(3770)$ may be not a pure $c\bar{c}$ state or some unknown structure may exist in the energies around 3.773 GeV [6]. To search for the new structure, as suggested in Ref. [6], we studied the processes $e^+e^- \rightarrow J/\psi X$ ($X = \pi^+\pi^-, \pi^0\pi^0, \eta, \pi^0, \gamma\gamma$) in the energy region between 3.645 and 3.891 GeV.

In this Letter, we report a measurement of the observed cross sections of $e^+e^- \rightarrow J/\psi X$ based on 3.21 fb^{-1} of data taken with the BESIII [17] detector at the BEPCII [17] collider at 69 c.m. energies ranging from 3.645 to 3.891 GeV. These data correspond to integrated luminosity of 72 pb^{-1} of cross-section scan data [18] taken at energies from 3.645 to 3.891 GeV, 44.5 pb^{-1} taken at 3.650 GeV, 162.8 pb^{-1} taken at 3.6861 GeV [19], 2.93 fb^{-1} taken at 3.773 GeV [20], and 50.5 pb^{-1} taken at 3.808 GeV.

The BESIII detector and its response are described elsewhere [21]. Here, we discuss only those aspects that are specifically related to this study. The production of the $\psi(3686)$ and $\psi(3770)$ resonances are simulated with the Monte Carlo (MC) event generator KKMC [22]. The decays of these resonances to $J/\psi\pi^+\pi^-$, $J/\psi\pi^0\pi^0$, $J/\psi\eta$, $J/\psi\pi^0$, and $\gamma\chi_{cJ}$ ($J=0,1,2$) are generated with EVTGEN [23] according to the known [24] relative branching ratios into these final states. To study possible backgrounds, MC samples of inclusive $\psi(3686)$ and $\psi(3770)$ decays, $e^+e^- \rightarrow (\gamma)J/\psi$, $e^+e^- \rightarrow (\gamma)\psi(3686)$, $e^+e^- \rightarrow q\bar{q}$ ($q = u, d, s$), and other final states which may be misidentified as $J/\psi X$ are also generated. Here, γ in parentheses denotes the inclusion of photons from the initial state radiation (ISR).

The observed cross section is determined with

$$\sigma^{\text{obs}}(e^+e^- \rightarrow J/\psi X) = \frac{N^{\text{obs}} - N_b}{\mathcal{L}\epsilon\mathcal{B}(J/\psi \rightarrow \ell^+\ell^-)} \quad (1)$$

at c.m. energy \sqrt{s} , where N^{obs} and N_b are, respectively, the number of $J/\psi X$ events obtained from the data and the number of background events estimated by MC simulations, \mathcal{L} is the integrated luminosity of the data, ϵ is the efficiency for the selection of $e^+e^- \rightarrow J/\psi X$ events, and $\mathcal{B}(J/\psi \rightarrow \ell^+\ell^-)$ is the branching fraction for J/ψ decays to the lepton pair $\ell^+\ell^-$.

The J/ψ is reconstructed via the e^+e^- and $\mu^+\mu^-$ final states. Each event is required to have exactly two charged tracks and more than one photon or to have three or four charged tracks in the final state. For each charged track, the polar angle θ in the multilayer drift chamber (MDC) must satisfy $|\cos\theta| < 0.93$. For all charged tracks, the distance of closest approach to the average e^+e^- interaction point is required to be less than 1.0 cm in the plane perpendicular to the beam and less than 10.0 cm along the beam direction. The electron and the muon can be well separated with the ratio E/p , where E is the energy deposited in the electromagnetic calorimeter (EMC) and p is the momentum of the charged track, which is measured using the information in the MDC. For e^\pm candidates, the ratio E/p is required to be larger than 0.7, while for μ^\pm , it is required to be in the range from 0.05 to 0.35. To reject radiative Bhabha scattering events, the polar angles of the leptons are required to satisfy $|\cos\theta| < 0.81$ and the angle between the two leptons to be less than 179° . The momenta of the leptons are required to be larger than 1 GeV and less than $0.47 \times E_{\text{c.m.}}$. To select π^\pm and to reject backgrounds such as $\pi^+\pi^-K^+K^-$ from $c\bar{c}$ and non- $c\bar{c}$ state decays and two-photon exchange processes of $e^+e^- \rightarrow \ell^+\ell^-K^+K^-$, the confidence level of the pion hypothesis, calculated based on dE/dx and time-of-flight measurements, is required to be greater than that of the corresponding kaon hypothesis. For the selection of photons, the deposited energy of a neutral cluster in the EMC is required to be greater than 25 MeV in the barrel and 50 MeV in the end caps. Time information from the EMC is used to suppress electronic noise and energy deposits unrelated to the event. To exclude fake photons originating from charged tracks, the angle between the photon candidate and the nearest charged track is required to be greater than 10° . The $J/\psi X$ is reconstructed with the selected tracks and photons.

The number of $J/\psi X$ candidates is determined by fitting the $\ell^+\ell^-$ invariant mass spectra of the events satisfying the previously described selection criteria. This is illustrated in Fig. 1, which shows two $\ell^+\ell^-$ invariant mass spectra from the scan data. The J/ψ resonance is clearly observed. We fit these mass spectra with a function describing both the signal and background shapes. The signal shape is described by the MC-simulated signal shape, while the

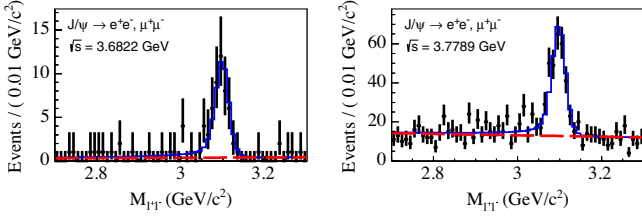


FIG. 1. The invariant-mass distributions of the $\ell^+\ell^-$ pair selected from data taken at two c.m. energies \sqrt{s} , where the dots with error bars are the number of the observed events, and the blue solid lines are the fit to these events, while the dashed red lines show the background.

smooth background is modeled by a linear function. The fits yield the numbers of the candidates for $e^+e^- \rightarrow J/\psi X$.

These selected candidate events still contain some background events, originating from several sources, which includes (i) $e^+e^- \rightarrow (\gamma)e^+e^-$, (ii) $e^+e^- \rightarrow (\gamma)\mu^+\mu^-$, (iii) $e^+e^- \rightarrow (\gamma)\tau^+\tau^-$, (iv) $e^+e^- \rightarrow (\gamma)D^+D^-$, (v) $e^+e^- \rightarrow (\gamma)D^0\bar{D}^0$, (vi) continuum light hadron production, and (vii) $e^+e^- \rightarrow (\gamma)J/\psi$ events. Detailed MC studies of these backgrounds show that only $e^+e^- \rightarrow (\gamma)J/\psi \rightarrow (\gamma)\ell^+\ell^-$ can be misidentified as $e^+e^- \rightarrow J/\psi X$, which is due to picking up fake photons or unphysical charged track(s). From these MC studies, we find that the fraction of these background events misidentified as signal events is $\eta_{\text{mis}} = (0.18 \pm 0.02)\%$. With the J/ψ resonance parameters [24]] as inputs and considering the energy spread, we extract the cross section $\sigma_{e^+e^- \rightarrow (\gamma)J/\psi}^{\text{ISR}}(\sqrt{s})$ for $e^+e^- \rightarrow (\gamma)J/\psi$, which includes both the ISR and vacuum polarization effects, and we determine $N_b = \mathcal{L}\sigma_{e^+e^- \rightarrow (\gamma)J/\psi}^{\text{ISR}}(\sqrt{s})\eta_{\text{mis}}$. For example, for the data shown in Fig. 1 (right), $\sigma_{e^+e^- \rightarrow (\gamma)J/\psi}^{\text{ISR}}(\sqrt{s})|_{\sqrt{s}=3.7789 \text{ GeV}} = 0.99 \pm 0.04 \text{ nb}$, $\mathcal{L} = 1956.84 \pm 4.65 \text{ nb}^{-1}$, and $N_b = 3.5 \pm 0.4$.

The efficiencies for the selection of $e^+e^- \rightarrow J/\psi X$ decays are determined with MC simulated events for these decays including the ISR and final-state radiative effects, where the final states include $J/\psi\pi^+\pi^-$, $J/\psi\pi^0\pi^0$, $J/\psi\eta$, $J/\psi\pi^0$, and $\gamma\chi_{cJ}$ ($J=0, 1, 2$) in which $\chi_{cJ} \rightarrow \gamma J/\psi$ followed by $J/\psi \rightarrow e^+e^-$ and $J/\psi \rightarrow \mu^+\mu^-$. All decay branching fractions are taken from the Particle Data Group [24]. With the MC samples generated at 69 c.m. energies ranging from 3.645 to 3.895 GeV, we determine the corresponding efficiencies. We observe an energy-dependent efficiency curve increasing smoothly from 58.8% at 3.645 GeV to 60.8% at 3.891 GeV.

With the numbers of candidates for $e^+e^- \rightarrow J/\psi X$ selected from the 69 datasets, N_b , \mathcal{L} , $\epsilon_{J/\psi X}$, and $\mathcal{B}(J/\psi \rightarrow \ell^+\ell^-)$, we determine the observed cross sections at these energies [25]. Table I shows the source of systematic uncertainty of the cross section. The total systematic uncertainty is 2.0%.

Figure 2 shows the observed cross sections as circles with error bars, where the errors are statistical uncertainties

TABLE I. Source of the systematic uncertainties of the observed cross section of $e^+e^- \rightarrow J/\psi X$.

Source	Uncertainty (%)
$\cos\theta$ cut	0.4
E/p cut	0.3
p_{T^\pm}	0.2
Cut on number of charged tracks or photons	0.4
Tracking efficiency for pions	0.3
Fitting the invariant-mass spectrum	0.8
Modeling of the MC	0.9
Identification of π^\pm	1.0
Uncertainty of $\mathcal{B}(J/\psi \rightarrow l^+l^-)$	0.4 [24]
Background subtraction	<0.1
Luminosity measurements	1.0
Total	2.0

on the observed cross section measurements. The dominant peak located at ~ 3.686 GeV is due to $\psi(3686)$ decays. The shape of the cross sections at energies above 3.72 GeV is not monotonic, indicating that there could be additional structure at energies between 3.72 and 3.87 GeV similar to the structure [4] observed by the BES Collaboration.

We analyze the cross sections by performing least- χ^2 fits to the cross sections. The expected cross section is modeled with

$$\sigma^{\text{exp}}(s) = \int_{\sqrt{s_-}}^{\sqrt{s_+}} dw \mathcal{G}(s, w) \int_0^{1-(M_{J/\psi}^2/s)} dx \sigma^{\text{dress}}(s') \mathcal{F}(x, s), \quad (2)$$

where x is the energy fraction of the radiative photon [26], $s' = s(1-x)$, $\mathcal{G}(s, w)$ [14] is a Gaussian function [27] describing the \sqrt{s} distribution of BEPCII, w integrates over the c.m. energy, $\sqrt{s}_\pm = \sqrt{s} \pm 5\Delta_{\text{sprd}}$, in which Δ_{sprd} is the

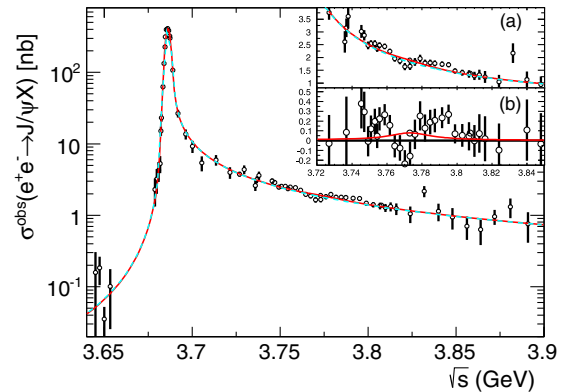


FIG. 2. The observed cross sections for $e^+e^- \rightarrow J/\psi X$ and the best fit to the cross sections under the assumption that the $\psi(3686)$ and $\psi(3770)$ decays contribute to the cross sections, where the insets show the enlargement of the subtle region (see the text for details).

energy spread, $\sigma^{\text{dress}}(s')$ is the dressed cross section including vacuum polarization effects for the $J/\psi X$ production, $M_{J/\psi}$ is the mass of J/ψ , and $\mathcal{F}(x, s)$ is a sampling function [26]. We perform the least- χ^2 fits to the cross sections under the two hypotheses discussed below.

Hypothesis A.—Assuming only $\psi(3686)$ and $\psi(3770)$ contributing of the cross sections, we fit the cross sections with inserting $\sigma^{\text{dress}}(s') = |A_{\psi(3686)}(s') + e^{i\phi_1} A_{\psi(3770)}(s')|^2$ into Eq. (2), where ϕ_1 is a phase, $A_{\psi(3686)}(s')$ and $A_{\psi(3770)}(s')$ are the generic decay amplitudes parameterized by a relativistic BW (RBW) function $A_j(s') = \sqrt{12\pi\Gamma_j^{ee}\Gamma_j^{\text{tot}}\mathcal{B}_j}/[(s' - M_j^2) + iM_j\Gamma_j^{\text{tot}}]$, in which the subscript j indicates one of these resonances, and M_j , Γ_j^{ee} , Γ_j^{tot} , and \mathcal{B}_j represent, respectively, the mass, leptonic width, total width, and decay branching fraction to $J/\psi X$ of the resonance. In this fit, the total and leptonic widths of both the $\psi(3686)$ and $\psi(3770)$ resonances and the mass of the $\psi(3770)$ resonance are fixed to the values given by the Particle Data Group [24], while the mass of $\psi(3686)$ and the branching fractions for the decays of $\psi(3686) \rightarrow J/\psi X$ and $\psi(3770) \rightarrow J/\psi X$ as well as the phase ϕ_1 are left as free parameters. The fit has two solutions with an identical fit $\chi^2 = 120.4$ for 64 degrees of freedom, which gives $\mathcal{B}(\psi(3686) \rightarrow J/\psi X) = (64.4 \pm 0.6 \pm 1.6)\%$, $\mathcal{B}(\psi(3770) \rightarrow J/\psi X) = (0.5 \pm 0.2 \pm 0.1)\%$, and $\phi_1 = (93 \pm 52 \pm 7)^\circ$ for solution I, where the first uncertainty value results from the fit and the second uncertainty value is of systematic origin. Solution II gives $\mathcal{B}(\psi(3686) \rightarrow J/\psi X) = (64.6 \pm 0.6 \pm 1.6)\%$, $\mathcal{B}(\psi(3770) \rightarrow J/\psi X) = (2.2 \pm 0.4 \pm 0.6)\%$, and $\phi_1 = (-105 \pm 24 \pm 8)^\circ$. The systematic uncertainties on these values have four sources for $\mathcal{B}(\psi(3686) \rightarrow J/\psi X)$, $\mathcal{B}(\psi(3770) \rightarrow J/\psi X)$, and ϕ_1 , which are, respectively, (i) 2.4%, 2.4%, and 0.1% due to uncertainty of the observed cross sections, (ii) 0.1%, 9.5%, and 6.0% due to uncertainties of the fixed parameters, (iii) 0.6%, 27.3%, and 3.4% due to uncertainties on \sqrt{s} , and (iv) 0.0%, 0.7%, and 3.8% due to choosing either the RBW or nonrelativistic BW (nRBW) function as the decay amplitudes (see below). Adding these uncertainties in quadrature yields the total systematic uncertainties. We choose solution I as the nominal results of the analysis, in which the $\psi(3770)$ decay branching fraction is consistent within its uncertainty with the sum of published branching fractions, $(0.47 \pm 0.06)\%$ [24], of $\psi(3770) \rightarrow J/\psi\pi^+\pi^-$, $J/\psi\pi^0\pi^0$, $J/\psi\eta$, and $\gamma\chi_J$ with $J = 0, 1, 2$. The branching fraction from solution II is larger than the total branching fraction in Ref. [24] by a factor of about 4. The solid line in Fig. 2 shows the fit result, while the dashed line shows the contribution from $\psi(3686) \rightarrow J/\psi X$ decays. To clearly see the significant variation of the cross sections at the energies around 3.773 GeV, we enlarge the partial cross-section data at energies from 3.72 to 3.85 GeV. The inset Fig. 2(a) shows the cross sections with the fit, while the inset

Fig. 2(b) shows the cross sections with the fit, for which the $\psi(3686)$ contribution is subtracted. The solid line in Fig. 2(b) corresponds to the fit result of the cross sections taking into account the $\psi(3770)$ decay and interference effects between the $\psi(3686)$ and $\psi(3770)$ decay amplitudes. It is clearly illustrated that the fit does not provide a good description of the cross-section data at energies above 3.72 GeV, indicating that some unknown structure \mathcal{S} may exist in this energy region.

Hypothesis B.—To search for the unknown structure \mathcal{S} , we fit the cross sections with inserting $\sigma^{\text{dress}}(s') = |A_{\psi(3686)}(s') + e^{i\phi_1} A_{\psi(3770)}(s')^2 + e^{i\phi_2} A_{\mathcal{S}}(s')|^2$ into Eq. (2), where ϕ_2 is a phase and $A_{\mathcal{S}}$ is the decay amplitude of the \mathcal{S} , which is also parameterized by a RBW function $A_{\mathcal{S}}(s')$ as that used in Hypothesis A. Compared to Hypothesis A, the fit has four additional free parameters: $M_{\mathcal{S}}$, $\Gamma_{\mathcal{S}}^{\text{tot}}$, $\Gamma_{\mathcal{S}}^{ee}\mathcal{B}_{\mathcal{S}}$, and ϕ_2 . The fit has four solutions. However, two of the solutions almost overlap with the other two, as expected according to mathematical predictions reported in Ref. [28]. The two fits have identical $\chi^2 = 82.6$ for 60 degrees of freedom. Table II summarizes the results returned from the fits, where the first uncertainty value reflects the fit result and the second uncertainty value is of systematic origin. We choose solution II as the nominal results of the analysis, because for the common parameters it is closer to the solution selected for Hypothesis A. Solution II gives $M_{\mathcal{S}} = 3766.2 \pm 3.8 \pm 0.4 \text{ MeV}/c^2$, $\Gamma_{\mathcal{S}} = 22.2 \pm 5.9 \pm 1.4 \text{ MeV}$, and $\Gamma_{\mathcal{S}}^{ee}\mathcal{B}(\mathcal{S} \rightarrow J/\psi X) = 79.4 \pm 85.5 \pm 11.7 \text{ eV}$. The large uncertainties on $\mathcal{B}(\psi(3770) \rightarrow J/\psi X)$ and $\Gamma_{\mathcal{S}}^{ee}\mathcal{B}(\mathcal{S} \rightarrow J/\psi X)$ are due to parameter correlations. The correlation coefficients between $\Gamma_{\mathcal{S}}^{ee}\mathcal{B}(\mathcal{S} \rightarrow J/\psi X)$ and $\mathcal{B}(\psi(3770) \rightarrow J/\psi X)$ and between $\mathcal{R}(3760)M_{\mathcal{S}}$ and $\mathcal{B}(\psi(3770) \rightarrow J/\psi X)$ are, respectively, 0.959 and 0.744. Figure 3 illustrates the fit to the cross sections, where

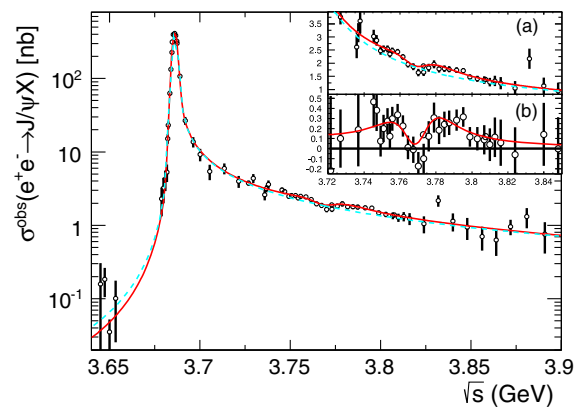


FIG. 3. The observed cross sections for $e^+e^- \rightarrow J/\psi X$ and the best fit to the cross sections under the assumption that the $\psi(3686)$, \mathcal{S} , and $\psi(3770)$ decays contribute to the cross sections. The insets show the enlargement of the subtle region in which the structure \mathcal{S} decaying into $J/\psi X$ is clearly seen (see the text for details).

the solid line shows the fit and the dashed line shows the contribution from $\psi(3686) \rightarrow J/\psi X$ decays, while the inset Fig. 3(a) shows the enlarged cross sections with the fit and the inset Fig. 3(b) shows the cross sections with the fit, for which the $\psi(3686)$ contribution is subtracted. The significant variation of the cross sections shown in Fig. 3(b) clearly illustrates that two BW decay amplitudes contribute to these cross sections. We denote \mathcal{S} as $\mathcal{R}(3760)$. The mass and total width of the $\mathcal{R}(3760)$ measured in this work are consistent within uncertainties with those [4] measured earlier by the BES Collaboration. Comparing to the fit $\chi^2 = 120.4$ for 64 degrees of freedom from the fit performed under Hypothesis A, increasing four free parameters in the fit causes the fit χ^2 reduced by 37.8, corresponding to the $\mathcal{R}(3760)$ signal significance of 5.3σ .

The parametrization of the resonance slightly affects the fitted results. Replacing the RBW with the nRBW function $A_k(s') = 1/M_k \sqrt{3\pi} \Gamma_k^{ee} \Gamma_k^{\text{tot}} \mathcal{B}_k / [(\sqrt{s'} - M_k) + i(\Gamma_k^{\text{tot}}/2)]$ for resonance k , the magnitudes of the fitted parameters for Hypothesis A change at the level of 10^{-6} to 3.8×10^{-2} , while these change under Hypothesis B at the level of 10^{-6} to 2.7×10^{-3} . We take the relative shift of the magnitude of a parameter as a measure of its corresponding systematic uncertainty due to the different parametrization of the resonance.

The systematic uncertainties in the fitted parameters presented in Table II are assumed to originate from four sources: (i) the uncertainty of the observed cross sections, (ii) the uncertainties of the fixed resonance parameters, (iii) the uncertainties of the c.m. energies, and (iv) the parametrization of the resonance. To estimate these uncertainties, we change the values of the cross sections and the fixed parameters by $\pm 1\sigma$, refit the observed cross sections, and subsequently take the difference between the refitted parameter value and the one of the nominal fit result as the corresponding systematic shift. A similar procedure has

TABLE II. The fitted results, where $M_{\mathcal{R}_i}$, $\Gamma_{\mathcal{R}_i}^{\text{tot}}$, and $\Gamma_{\mathcal{R}_i}^{ee}$ are, respectively, the mass (MeV/ c^2), total width (MeV), and leptonic width (eV) of \mathcal{R}_i . $\mathcal{B}(\mathcal{R}_i \rightarrow f)$ ($f = J/\psi X$) is the decay branching fraction (%) of the \mathcal{R}_i , where $i = 1, 2, 3$ indicate, respectively, $\psi(3686)$, $\psi(3770)$, and $\mathcal{R}(3760)$. ϕ_1 and ϕ_2 are the phases (degree).

Parameter	Solution I	Solution II
$\mathcal{B}(\mathcal{R}_1 \rightarrow f)$	$62.8 \pm 0.6 \pm 1.7$	$62.3 \pm 0.8 \pm 1.6$
$M_{\mathcal{R}_2}$	3773.13	3773.13
$\Gamma_{\mathcal{R}_2}^{\text{tot}}$	27.2	27.2
$\mathcal{B}(\mathcal{R}_2 \rightarrow f)$	$55.1 \pm 36.2 \pm 6.3$	$38.1 \pm 41.4 \pm 4.3$
ϕ_1 (degree)	$175 \pm 30 \pm 30$	$60 \pm 37 \pm 10$
$M_{\mathcal{R}_3}$	$3766.2 \pm 3.1 \pm 0.4$	$3766.2 \pm 3.8 \pm 0.4$
$\Gamma_{\mathcal{R}_3}^{\text{tot}}$	$22.1 \pm 5.2 \pm 1.4$	$22.2 \pm 5.9 \pm 1.4$
$\Gamma_{\mathcal{R}_3}^{ee} \mathcal{B}(\mathcal{R}_3 \rightarrow f)$	$110.2 \pm 134.4 \pm 16.2$	$79.4 \pm 85.5 \pm 11.7$
ϕ_2	$322 \pm 34 \pm 30$	$213 \pm 48 \pm 20$

been applied to estimate the systematic error related to uncertainties on the c.m. energies. In this case, we vary the c.m. energies with a Gaussian uncertainty of 0.25 MeV in the resonance energy region, refit the data, and take the difference of the updated fit parameter value with respect to the result of the nominal fit as a measure of the systematic shift. Adding these uncertainties in quadrature yields the total systematic uncertainty for each parameter.

In summary, we have measured for the first time the observed cross sections of $e^+e^- \rightarrow J/\psi X$ at c.m. energies from 3.645 to 3.891 GeV. We fitted the cross sections with the sum of the known $\psi(3686)$ and $\psi(3770)$ states and obtained measurements of $\mathcal{B}(\psi(3686) \rightarrow J/\psi X) = (64.4 \pm 0.6 \pm 1.6)\%$ and $\mathcal{B}(\psi(3770) \rightarrow J/\psi X) = (0.5 \pm 0.2 \pm 0.1)\%$ for the first time. The fit quality can be improved by adding one more structure $\mathcal{R}(3760)$ in the fits. For the mass, total width, and product of the leptonic width and decay branching fraction of $\mathcal{R}(3760)$, the fit yields $M_{\mathcal{R}(3760)} = 3766.2 \pm 3.8 \pm 0.4 \text{ MeV}/c^2$, $\Gamma_{\mathcal{R}(3760)} = 22.2 \pm 5.9 \pm 1.4 \text{ MeV}/c^2$, and $\Gamma_{\mathcal{R}(3760)}^{ee} \mathcal{B}(\mathcal{R}(3760) \rightarrow J/\psi X) = 79.4 \pm 85.5 \pm 11.7 \text{ eV}$. The statistical significance of the $\mathcal{R}(3760)$ is 5.3σ . The mass and total width of the $\mathcal{R}(3760)$ are in very good agreement with the mass $M_{\mathcal{R}(3760)} = 3762.6 \pm 11.8 \pm 0.5 \text{ MeV}/c^2$ and total width $\Gamma_{\mathcal{R}(3760)} = 49.9 \pm 32.1 \pm 0.1 \text{ MeV}/c^2$ of $R(3760)$ [4] observed in $e^+e^- \rightarrow \text{hadrons}$ by the BES Collaboration at the BES-II experiment.

The BESIII Collaboration thank the staff of BEPCII and the IHEP computing center for their strong support. This work is supported in part by National Key Basic Research Program of China under Contracts No. 2009CB825204 and No. 2015CB856700; National Key R&D Program of China under Contract No. 2020YFA0406400; National Natural Science Foundation of China (NSFC) under Contracts No. 10935007, No. 11625523, No. 11635010, No. 11735014, No. 11822506, No. 11835012, and No. 11961141012; the Chinese Academy of Sciences (CAS) Large-Scale Scientific Facility Program; Joint Large-Scale Scientific Facility Funds of the NSFC and CAS under Contracts No. U1532257, No. U1532258, No. U1732263, and No. U1832207; CAS Key Research Program of Frontier Sciences under Contracts No. QYZDJ-SSW-SLH003 and No. QYZDJ-SSW-SLH040; 100 Talents Program of CAS; CAS Other Research Program under Code No. Y129360; INPAC and Shanghai Key Laboratory for Particle Physics and Cosmology; ERC under Contract No. 758462; German Research Foundation DFG under Contracts No. Collaborative Research Center CRC 1044 and No. FOR 2359; Istituto Nazionale di Fisica Nucleare, Italy; Ministry of Development of Turkey under Contract No. DPT2006K-120470; National Science and Technology fund; STFC (United Kingdom); The Knut and Alice Wallenberg Foundation (Sweden) under Contract No. 2016.0157; The Royal Society, United Kingdom under

Contracts No. DH140054 and No. DH160214; The Swedish Research Council; and U.S. Department of Energy under Contracts No. DE-FG02-05ER41374, No. DE-SC-0010118, and No. DE-SC-0012069.

^aAlso at Ankara University, 06100 Tandogan, Ankara, Turkey.

^bAlso at Bogazici University, 34342 Istanbul, Turkey.

^cAlso at the Moscow Institute of Physics and Technology, Moscow 141700, Russia.

^dAlso at the Functional Electronics Laboratory, Tomsk State University, Tomsk 634050, Russia.

^eAlso at the Novosibirsk State University, Novosibirsk 630090, Russia.

^fAlso at the NRC “Kurchatov Institute”, PNPI, Gatchina 188300, Russia.

^gAlso at Istanbul Arel University, 34295 Istanbul, Turkey.

^hAlso at Goethe University Frankfurt, 60323 Frankfurt am Main, Germany.

ⁱAlso at Key Laboratory for Particle Physics, Astrophysics and Cosmology, Ministry of Education; Shanghai Key Laboratory for Particle Physics and Cosmology; Institute of Nuclear and Particle Physics, Shanghai 200240, People’s Republic of China.

^jAlso at Key Laboratory of Nuclear Physics and Ion-beam Application (MOE) and Institute of Modern Physics, Fudan University, Shanghai 200443, People’s Republic of China.

^kAlso at Department of Physics, Harvard University, Cambridge, Massachusetts 02138, USA.

^lPresent address: Institute of Physics and Technology, Peace Avenue 54B, Ulaanbaatar 13330, Mongolia.

^mAlso at State Key Laboratory of Nuclear Physics and Technology, Peking University, Beijing 100871, People’s Republic of China.

ⁿAlso at School of Physics and Electronics, Hunan University, Changsha 410082, China.

- [1] G. Rong, in *Proceedings of the Symposium of 30 Years of BES Physics, Beijing, China* (World Scientific, Singapore, 2019), p. 48.
- [2] M. Ablikim *et al.* (BESIII Collaboration), *Phys. Rev. D* **102**, 112009 (2020).
- [3] J. Z. Bai *et al.* (BES Collaboration), [arXiv:hep-th/0307028](https://arxiv.org/abs/hep-th/0307028); G. Rong and D. G. Cassel, in *Proceedings of Tenth International Conference on Hadron Spectroscopy, Aschaffenburg, Germany* (American Institute of Physics, Melville, 2004), pp. 592–600; J. Z. Bai *et al.* (BES Collaboration), *Chin. Phys. C* **28**, 325 (2004); *Phys. Lett. B* **605**, 63 (2005).
- [4] M. Ablikim *et al.* (BES Collaboration), *Phys. Rev. Lett.* **101**, 102004 (2008).
- [5] M. Ablikim *et al.* (BESIII Collaboration), *Phys. Rev. D* **102**, 112009 (2020).
- [6] G. Rong, *Chin. Phys. C* **34**, 788 (2010).
- [7] M. Ablikim *et al.* (BES Collaboration), *Phys. Rev. D* **91**, 092009 (2015).
- [8] S.-K. Choi *et al.* (Belle Collaboration), *Phys. Rev. Lett.* **91**, 262001 (2003).
- [9] B. Aubert *et al.* (BABAR Collaboration), *Phys. Rev. Lett.* **95**, 142001 (2005).
- [10] M. Ablikim *et al.* (BESIII Collaboration), *Phys. Rev. Lett.* **118**, 092001 (2017).
- [11] M. Ablikim *et al.* (BESIII Collaboration), *Phys. Rev. Lett.* **118**, 092002 (2017).
- [12] E. Eichten, K. Gottfried, T. Kinoshita, K. D. Lane, and T.-M. Yan, *Phys. Rev. D* **17**, 3090 (1978).
- [13] M. Ablikim *et al.* (BES Collaboration), *Phys. Lett. B* **641**, 145 (2006).
- [14] M. Ablikim *et al.* (BES Collaboration), *Phys. Rev. Lett.* **97**, 121801 (2006).
- [15] M. Ablikim *et al.* (BES Collaboration), *Phys. Rev. D* **76**, 122002 (2007).
- [16] M. Ablikim *et al.* (BES Collaboration), *Phys. Lett. B* **659**, 74 (2008).
- [17] M. Ablikim *et al.* (BESIII Collaboration), *Nucl. Instrum. Methods Phys. Res., Sect. A* **614**, 345 (2010).
- [18] M. Ablikim *et al.* (BESIII Collaboration), *Chin. Phys. C* **42**, 063001 (2018).
- [19] M. Ablikim *et al.* (BESIII Collaboration), *Chin. Phys. C* **41**, 063001 (2017).
- [20] M. Ablikim *et al.* (BESIII Collaboration), *Phys. Lett. B* **753**, 629 (2016).
- [21] M. Ablikim *et al.* (BESIII Collaboration), *Nucl. Instrum. Methods Phys. Res., Sect. A* **614**, 345 (2010).
- [22] S. Jadach, B. F. L. Ward, and Z. Was, *Comput. Phys. Commun.* **130**, 260 (2000).
- [23] D. J. Lange, *Nucl. Instrum. Methods Phys. Res., Sect. A* **462**, 152 (2001); R.-G. Ping, *Chin. Phys. C* **32**, 599 (2008).
- [24] M. Tanabashi *et al.* (Particle Data Group), *Phys. Rev. D* **98**, 030001 (2018).
- [25] See Supplemental Material at <http://link.aps.org/supplemental/10.1103/PhysRevLett.127.082002> for the numerical cross sections.
- [26] E. A. Kuraev and V. S. Fadin, *Yad. Fiz.* **41**, 377 (1985) [*Sov. J. Nucl. Phys.* **41**, 466 (1985)].
- [27] M. Ablikim *et al.* (BES Collaboration), *Phys. Lett. B* **652**, 238 (2007).
- [28] Y. Bai and D.-Y. Chen, *Phys. Rev. D* **99**, 072007 (2019); K. Zhu, X. H. Mo, C. Z. Yuan, and P. Wang, *Int. J. Mod. Phys. A* **26**, 4511 (2011).